Energy Engineering

Tech Science Press

Doi:10.32604/ee.2025.072860

ARTICLE

Optimal Scheduling of Integrated Energy Systems with P2G-CCS Coupling and Hydrogen-Blended Natural Gas under Tiered Carbon Trading

Yansen Sun[1,2], Yi Ding[3], Hualei Cui[4], Yuanchao Hui[5] and Yupeng He[1,2,*]

[1]Key Laboratory of Modern Power System Simulation and Control & Renewable Energy Technology, Ministry of Education, Northeast Electric Power University, Jilin, 132012, China
[2]Department of Electrical Engineering, Northeast Electric Power University, Jilin, 132012, China
[3]Zhejiang Zheneng Zhongmei Zhoushan Coal Power Co., Ltd., Zhoushan, 316131, China
[4]State Grid Weihui Power Supply Company, Xinxiang, 453100, China
[5]Ultra-High Voltage Company of State Grid Henan Electric Power Company, Nanyang, 473000, China

*Corresponding Author: Yupeng He. Email: 18943290602@163.com

Received: 05 September 2025; Accepted: 28 October 2025; Published: 18 June 2026

ABSTRACT: Integrated energy systems (IES) are pivotal for achieving low-carbon transitions, yet their optimization under carbon constraints remains challenging. This paper proposes an optimal scheduling model for IES that synergistically combines power-to-gas coupled with carbon capture systems (P2G-CCS) and hydrogen-blended natural gas under a tiered carbon trading mechanism. The model innovatively refines the P2G process into two stages (electrolysis and methanation), utilizing methanation reaction heat to enhance efficiency. It further incorporates hydrogen blending into gas turbines and boilers and implements a tiered carbon trading mechanism to constrain emissions. The objective is to minimize total costs, including carbon trading, fuel procurement, carbon capture, unit cycling, and wind curtailment penalties. The model is linearized and solved using MATLAB/YALMIP with the CPLEX solver. Comparative simulation results demonstrate the significant advantages of the proposed strategy: it reduces the total operating cost by 7.69%, cuts carbon emissions by 7.3%, and lowers wind curtailment costs by 20.16% compared to a uniform carbon trading benchmark. Furthermore, analysis of hydrogen blending ratios reveals that a dynamic blending strategy can reduce gas turbine output and electrolysis power consumption by 6.88% and 20.93%, respectively, compared to a fixed-ratio approach. The study confirms that the deep coupling of P2G-CCS, flexible hydrogen utilization, and the tiered carbon market collectively enhance the low-carbon economic performance of IES.

KEYWORDS: Integrated energy system; P2G-CCS; hydrogen blending in natural gas; tiered carbon trading

1 Introduction

To advance towards a green, low-carbon, and renewable energy-dominated era, the dual-carbon goals were officially established by China, mandating national carbon emissions to reach their apex by 2030 followed by full carbon neutrality implementation before 2060, accompanied by a comprehensive carbon peaking and neutrality action plan [1]. As energy system reforms and energy-saving initiatives progress, one of the important strategies for accomplishing these dual-carbon goals is integrated energy system (IES), leveraging their multi-energy complementarity to underpin sustainable, low-carbon economic development.

Concurrently, profound transformations in global energy markets present both opportunities and challenges for the optimal operation of IES. On the one hand, the electricity market is rapidly transitioning towards a high penetration of renewable energy [2]. The large-scale integration of intermittent sources

like wind and solar power has led to insufficient system flexibility, frequent curtailment, and severe price volatility. On the other hand, the natural gas market, as a crucial source of flexible energy, is becoming increasingly coupled with the electricity market [3]. Natural gas is not only used for power generation but its pipeline network also possesses significant energy storage potential. However, price volatility and supply security concerns in the natural gas market remain significant issues. Against this backdrop, leveraging technological solutions to break down the barriers between electricity and gas sectors, mitigate renewable energy fluctuations, and simultaneously hedge against price risks in both markets has become a central task for the low-carbon economic dispatch of IES. The P2G-CCS coupling and hydrogen-blended natural gas technologies investigated in this paper constitute a comprehensive solution to this challenge: P2G converts surplus electricity into gas ("power-to-gas"), thereby smoothing power output and absorbing renewable curtailment; hydrogen-blended natural gas further enhances the decarbonization and flexibility of the gas network, creating new avenues for renewable energy accommodation.

Carbon capture and storage (CCS), a carbon-reducing technology, enables emission reductions in conventional thermal power plants by retrofitting existing coal- and gas-fired units. Reference [4] employs a multi-faceted approach to provide a comprehensive overview of the Technology Readiness Level assessment of existing CCS technologies, covering various types of CCS methods. To achieve low-carbon power systems, Reference [5] conducted a low-carbon economic dispatch model, including carbon capture and storage (CCS), two-stage power-to-gas (P2G), and combined heat and power (CHP) units, was constructed. Through setting multiple scenarios for case analysis, the effectiveness of the proposed model was verified. Reference [6] developed a hybrid carbon capture and storage approach combining membrane separation with amine absorption. This approach utilizes solar assistance to decarbonize fossil-based power generation in natural gas combined cycle plants while boosting power system sustainability and operational flexibility. In reference [7] a broad-learning prediction model for carbon emission balance in an integrated energy system was established. This model incorporates distributed ground-source heat pump thermal storage and carbon capture and storage. Simulation analyses demonstrate that the model reduces system carbon emissions, verifying its effectiveness. Reference [8] proposed a hybrid system integrating CCS, concentrated solar power, and combined heat and power (CHP), achieving significant carbon emission reduction through synergistic energy utilization. Reference [9] developed a system combining power-to-gas (P2G) and CCS technologies to enable efficient CO_2 capture and utilization. Reference [10] developed a coupling model between CCS and coal-fired CHP units, achieving both emission reductions and improved economic efficiency. Reference [11] developed a carbon capture, utilization, and storage (CCUS) method incorporating lean/rich solution storage tanks and a two-stage power-to-gas (P2G) system. This configuration facilitates the full absorption of renewable energy, broadens hydrogen utilization, and ultimately lowers operational costs. Although the aforementioned studies utilized CCS for emission reduction, they overlooked the coupling with P2G devices. The CO_2 captured by CCS could be synergistically utilized through integration with P2G, which holds significant implications for advancing low-carbon development in power systems.

On the technical coupling front, although references [4–10] delve into the flexible operation of CCS and its synergy with the system, and references [9–11] begin to explore the linkage between P2G and CCS, most treat P2G as a 'black-box' model, overlooking the energy flow characteristics of its internal two stages (hydrogen electrolysis and methanation) and the diverse utilization pathways for hydrogen. More critically, they fail to establish a complete 'capture-to-utilization' closed-loop carbon cycle, resulting in the final destination of CO_2 remaining storage rather than resource utilization.

The aforementioned literature analyzes the impact of CCS on system flexibility and low-carbon characteristics from both the CCS itself and its coupling with other units. However, existing studies on CCS coupled with P2G systems have overlooked the hydrogen production process in electrolysis, alternative

utilization pathways of hydrogen, and the low efficiency of methanation. A tiered carbon trading mechanism has not been incorporated into any of these studies. This paper proposes enhancing hydrogen utilization through hydrogen-blended natural gas. Regarding research on hydrogen blending in natural gas, Reference [12] investigated the modelling and simulation of integrated energy systems combining hydrogen-mixed natural gas and electricity, thereby improving renewable energy accommodation. Reference [13] developed simulation models to quantify the thermodynamic behaviors of natural gas-hydrogen fuel blends and assess their effects on internal combustion engine efficiency metrics. achieving economic cost optimization. Reference [14] demonstrated that blending hydrogen within 20% in gas turbines and boilers satisfies flame stability and combustion requirements. Reference [14] analyzes gas turbine combustion technologies for hydrogen mixtures, highlighting that hydrogen-enriched combustion can reduce system carbon emissions and stabilize grid operation. References [15,16] analyzed the energy efficiency of hydrogen-fueled gas turbine cycle systems and performed computational fluid dynamics (CFD) numerical simulations, summarizing combined cycle patterns for hydrogen-enriched gas turbines. While prior investigations encompassed CFD modeling and thermodynamic performance evaluations in gas turbine systems, they failed to consider multi-energy coupled systems from a macroscopic perspective. Reference [17] developed a Virtual Power Plant (VPP) system integrating P2G-CCS coupling with hydrogen-blended natural gas, evaluating how varying hydrogen blending proportions influence the VPP's low-carbon efficiency and economic feasibility. However, it did not fully utilize the reaction heat generated during the methanation stage of P2G.

In the realm of hydrogen utilization, references [12–15] provide valuable foundational research on the combustion characteristics and component-level performance of hydrogen-blended natural gas. Although reference [17] attempts a system-level analysis, its perspective remains largely confined to static or single blending modes. Research is scarce from the macroscopic perspective of IES global optimal dispatch that quantitatively analyzes the impact of dynamic, multi-path hydrogen utilization strategies on the system's carbon-economic performance.

As low-carbon development paradigms continue to evolve globally, emissions trading mechanisms have progressively established themselves as pivotal economic instruments for climate governance. Academic researchers have systematically investigated carbon market mechanisms. Reference [18] proposed that carbon trading policies facilitate the transition to a low-carbon economy, promote economic growth, and help achieve carbon reduction targets. Reference [19] integrated a carbon market framework into the IES, demonstrating both emission reductions and cost minimization via allowance trading. Addressing issues such as resource management, Reference [20] proposes a multi-objective optimization model. This model considers the integration of power-to-gas (P2G) and electric vehicle parking lots (EVPL), significantly reducing the operational costs and carbon emissions of both the natural gas network and the distribution grid. Although these studies incorporated carbon trading in their systems, they remained limited to uniform carbon trading models, failing to fully exploit the system's low-carbon potential.

Contemporary research has increasingly concentrated on multi-level carbon markets to more systematically assess systems' decarbonization capabilities. Reference [21] establishes a typical system framework involving various stakeholders and defines the energy and carbon market mechanisms. Simulation analysis demonstrates that the carbon trading mechanism can effectively constrain and reduce overall system carbon emissions. Reference [22] quantified the emission trading expenses of IES through emission factors and an incentive-punishment graded carbon pricing model, concurrently analyzing the cost-effectiveness of carbon capture facilities. Reference [23] proposed a carbon quota mechanism tailored to IES operational features and established a stepwise carbon trading pricing model to curb system emissions while facilitating low-carbon and economic operation. Reference [24] formulated a compensation pricing strategy for electric vehicles engaged in real-time economic scheduling within a carbon market framework, improving their energy

efficiency and emission-cutting advantages. These studies optimized the source-side structure of systems by integrating tiered carbon trading policies with low-carbon technologies, thereby improving emission reduction capabilities. However, no studies have systematically assessed the effects of varied carbon trading mechanisms on systems incorporating P2G-CCS coupled technologies.

Regarding market mechanisms, references [18–20,23,24] confirm the role of carbon trading in promoting a low-carbon economy, but they predominantly adopt a uniform carbon price. This mechanism provides insufficient incentive for deep decarbonization. Although references [21–23] introduce a tiered carbon trading mechanism, no study has yet systematically applied it to an IES coupled with the complex technological system of P2G-CCS and hydrogen-blended natural gas, to test its effectiveness in fully unleashing the emission reduction potential of this technology portfolio.

Despite significant progress in CCS, P2G, and hydrogen-blended natural gas, several limitations persist in the existing literature:

(1) Most studies have not fully explored the deep coupling between P2G and CCS, failing to establish a closed-loop "capture-utilization" carbon cycle. They often overlook alternative utilization pathways for electrolytic hydrogen (e.g., direct blending) and the overall system efficiency.
(2) Research on hydrogen-blended natural gas primarily focuses on combustion characteristics or component-level performance, lacking a macroscopic perspective from the Integrated Energy System (IES) optimal dispatch to analyze its synergistic carbon reduction and economic benefits.
(3) Regarding carbon trading mechanisms, existing works predominantly employ a uniform carbon price, which fails to fully exploit the strong incentivizing effect of a tiered carbon trading mechanism for deep decarbonization, especially its application in IES coupled with P2G-CCS.

To address these gaps, this paper proposes an optimal scheduling model for IES that integrates P2G-CCS coupling and hydrogen-blended natural gas under a tiered carbon trading mechanism. The main contributions of this work are threefold:

(1) Developing a two-stage P2G model (electrolysis and methanation) that utilizes the methanation reaction heat to improve overall energy utilization efficiency.
(2) Establishing operational models for gas turbines and boilers with hydrogen blending, quantitatively evaluating the impact of different blending ratios on system carbon emissions and economic performance.
(3) Incorporating a tiered carbon trading mechanism into this complex system to comprehensively assess its synergistic effects with P2G-CCS and hydrogen blending.

The proposed strategy's effectiveness is rigorously validated through comparative analysis across multiple operational scenarios, demonstrating its capability to enhance low-carbon performance while maintaining economic viability. This work advances the integration of policy-driven carbon constraints and multi-energy synergies in IES optimization.

2 Synergistic Architecture of IES with P2G-CCS and Hydrogen-Infused Gas Infrastructure

Fig. 1 depicts the structure of the integrated energy system in this paper. The system primarily obtains energy from power supply and gas supply systems, consisting of wind turbines, gas turbines, coal-fired units, two-stage power-to-gas units, gas boilers, carbon capture equipment, electric heating boilers, as well as electricity storage and thermal storage devices. Electricity demand is fulfilled through renewable energy sources, gas-fired turbines, and coal-based power plants. Heat demand is managed via gas turbine cogeneration, gas-fired boilers, and electric resistance heaters.

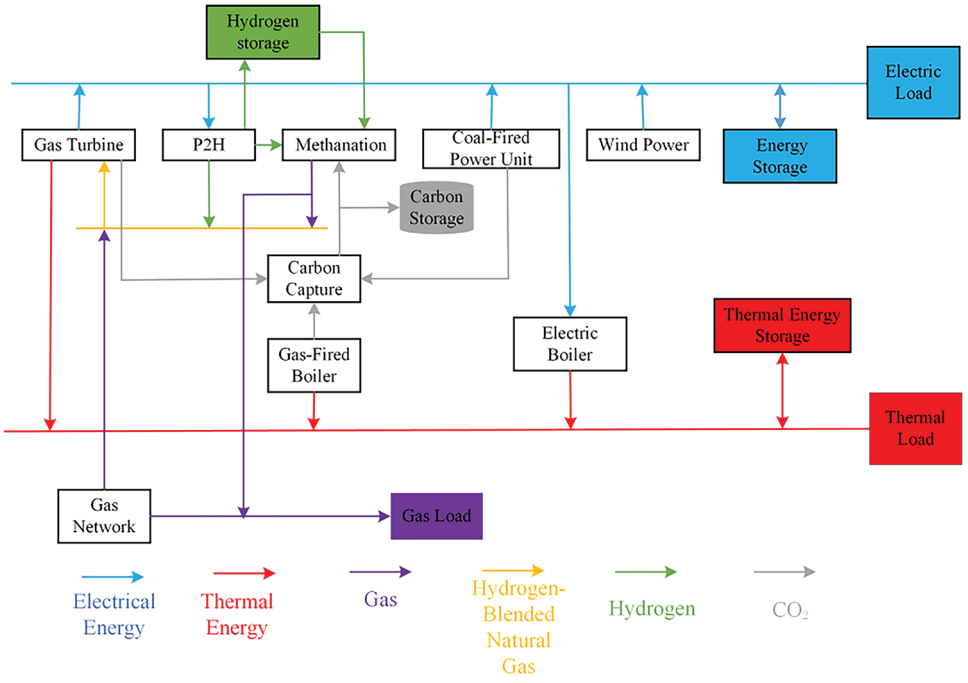

Figure 1: Integrated energy system structure diagram

3 Optimal Dispatch Model for IES Incorporating P2G-CCS Coupling and Hydrogen-Blended Natural Gas under Tiered Carbon Trading Mechanisms

Building on existing models, this study refines the Power-to-Gas (P2G) process into two distinct operational stages. To tackle system-level carbon emissions, a dual-strategy approach is implemented: carbon capture technology is used to sequester CO_2 emissions, with a portion redirected as feedstock for the P2G process to create an internal carbon cycle. Meanwhile, energy operators and consumers collaborate in carbon trading markets to enforce emission constraints. Additionally, hydrogen-blended combustion in gas turbines and boilers contributes to further emission reductions. The integrated system architecture, which includes the two-stage P2G process, carbon capture, and hydrogen-enriched combustion subsystems, is illustrated in Fig. 2.

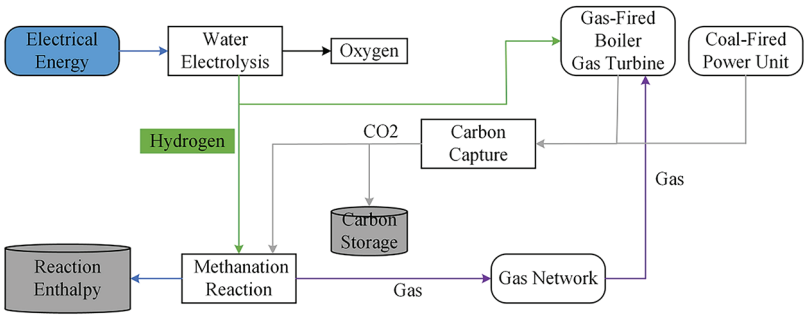

Figure 2: Structure of the two-stage P2G, CCS, and hydrogen-blended gas subsystem

The P2G system involves two consecutive phases: electrolysis-driven hydrogen generation and subsequent methane synthesis. In the initial stage, water electrolysis primarily occurs during periods of renewable energy surplus and lower electricity demand. A portion of the generated hydrogen is supplied to gas

turbines and boilers, while any surplus hydrogen proceeds to the next stage. The methanation phase converts hydrogen into methane through catalytic synthesis, and the resulting synthetic natural gas is injected into gas distribution networks. This staged implementation allows for precise energy conversion from electricity to gaseous fuels, improving energy utilization efficiency in integrated energy systems.

The P2G-CCS integrated system establishes a carbon cycle through coordinated operation: carbon capture technology recycles CO_2 emissions as feedstock for methanation, while hydrogen-enriched combustion in thermal units lowers carbon intensity. This synergistic configuration simultaneously addresses the efficiency limitations found in conventional P2G processes through optimized energy management.

3.1 The Integrated P2G-CCS Model

To explicitly address the novelty and practical value of the constructed model, the key differences and innovations compared to existing models are threefold:

A Closed-Loop Carbon Cycle within a Unified IES Framework: Unlike previous studies that treat P2G and CCS as separate entities or only partially couple them, our model establishes a deep, two-stage P2G-CCS coupling that creates a closed-loop "capture-utilization" carbon cycle. The captured CO_2 is not just stored but actively utilized as a feedstock for methane synthesis. This integrated architecture, which synergistically combines carbon capture, hydrogen production, methanation, and hydrogen blending within a single scheduling model, represents a significant step beyond the existing literature. It transforms CO_2 from a waste liability into a valuable resource, simultaneously reducing emissions and operational costs.

Dynamic Multi-Pathway Hydrogen Utilization Strategy: Existing models often limit hydrogen use to a single pathway. Our model innovates by introducing a flexible, multi-pathway hydrogen utilization strategy. The electrolytic hydrogen can be either directly injected into gas turbines and boilers for immediate decarbonization of heat and power generation, or it can be diverted to the methanation unit to produce substitute natural gas, enhancing grid flexibility. Furthermore, we model and optimize a time-varying hydrogen blending ratio, moving beyond the fixed-ratio assumptions common in prior work. This flexibility allows the system operator to dynamically decide the most economically and environmentally beneficial use of hydrogen in real-time, significantly improving operational efficiency and renewable energy absorption.

The practical application value of this model lies in its ability to provide a comprehensive and actionable decision-support tool for system operators and policymakers. It demonstrates a viable pathway for existing energy systems to transition towards low-carbon operation without sacrificing economic viability. By quantifying the synergies between key technologies and market mechanisms, our model can guide infrastructure investment inform the development of gas grid standards for hydrogen blending, and help policymakers design more effective carbon market regulations to accelerate the achievement of carbon neutrality goals.

3.1.1 CCS Model

The CCS system includes processes for capturing and storing carbon dioxide (CO_2). A fraction of the sequestered CO_2 is conveyed through carbon transport networks to Power-to-Gas plants for reutilization, with the residual CO_2 being pressurized and sequestered via dedicated compression units.

The energy consumption associated with the capture process includes both fixed and operational energy demands. The integration of CCS alters the configuration and operating conditions of traditional coal and gas-fired power units. Fixed energy consumption arises from efficiency losses in power generation, which remain constant regardless of whether CCS is operational. On the other hand, running energy expenditure includes the heat needed for CO_2 regeneration and the electricity employed during compression phases. This operational energy demand accounts for the majority of the energy required by CCS and varies based on the

operational status of the system [25].

$$\begin{cases} P_{CCS}(t) = P^{r}_{CCS}(t) + P^{s}_{CCS} \\ P^{r}_{CCS}(t) = \lambda_{GE}\eta_{C}e_{G}P_{G}(t) \\ E_{CC}(t) = \eta_{C}e_{G}P_{G}(t) \\ 0 \leqslant P_{CCS}(t) \leqslant P^{\max}_{CCS} \end{cases} \tag{1}$$

In the equation: $P_{CCS}(t)$ is the energy usage of the CCS unit throughout period t; $P^{r}_{CCS}(t)$ denotes the power demand of CCS operations during interval t; P^{s}_{CCS} defines the CCS system's base power consumption; $P_{G}(t)$ denotes the coal/gas-fired generation output at t; e_G is the carbon intensity of electricity generation; η_C indicates the CO_2 capture efficiency of CCS; λ_{GE} indicates the energy required per unit CO_2 captured; $P^{\max}_{CCS}$ specifies the maximum operational power limit of the CCS system.

Due to the significant energy costs associated with traditional carbon capture processes, this study introduces a CCS configuration that integrates flue gas splitting. This system effectively reduces the energy required for CO_2 capture by partially venting exhaust streams in a controlled manner. The operational principle of this approach can be expressed mathematically as follows:

$$E_{1}(t) = E(t) - e_{1}(t) \tag{2}$$

In the equation: $E(t)$ represents the total CO_2 emissions from generation units at time t; $E_1(t)$ denotes the CO_2 captured by CCS during period t; $e_1(t)$ corresponds to the CO_2 emission to the atmosphere through flue gas splitting at time t.

3.1.2 Two-Stage P2G Model

The P2G system incorporates wind energy by transforming it into storage-capable methane, enabling delivery to gas-utilizing devices in the IES when required. The operation of this system involves two main processes: electrolytic hydrogen production and methanation. In the methane synthesis stage, the CO_2 input quantity equates to the output volume of synthetic CH_4. The P2G model is defined as [26]:

$$\begin{cases} P^{Gas}_{P2G}(t) = \eta_{P2G}P^{e}_{P2G}(t) \\ V_{CO_2}(t) = V_{Gas}(t) = 3.6P^{Gas}_{P2G}(t)/H_{g} \\ E^{CO_2}_{P_2G}(t) = \rho_{CO_2}V_{CO_2}(t) \\ Q_{H2G,out}(t) = \eta_{H2G}Q_{H2G,in}(t) \end{cases} \tag{3}$$

In the equation: $P^{Gas}_{P2G}(t)$ signifies the natural gas power output of the P2G system in time interval t; $P^{e}_{P2G}(t)$ specifies the electrical power input required for P2G operation in period t; η_{P2G} represents the conversion efficiency of the P2G process; $V_{CO_2}(t)$ and $V_{Gas}(t)$ are the CO_2 absorption and natural gas production within period t; H_g indicates the calorific value of natural gas (39 MJ/m³); $E^{CO_2}_{P_2G}(t)$ quantifies the mass of CO_2 absorbed by P2G at t; ρ_{CO_2} is the density of CO_2; $Q_{H2G,out}(t)$ and $Q_{H2G,in}(t)$ denote the methane generation rate and H2 utilization rate at t; η_{H2G} denotes the methanation conversion efficiency.

3.2 Hydrogen-Blended Operation Model for Gas Turbines and Gas-Fired Boilers

Conventional micro gas turbines (MGTs) and gas-fired boilers predominantly utilize natural gas as the primary fuel source, with combustion byproducts containing greenhouse gas CO_2, contributing to elevated carbon emissions within integrated energy systems. Peer-reviewed research substantiates that controlled hydrogen enrichment in MGT combustors and boiler burners concurrently satisfies critical operational

constraints, including flame stability and flashback suppression, while enabling the decarbonization of thermal energy conversion processes.

The following is the mathematical framework for the gas turbine's hydrogen-blended operation [27]:

$$\begin{cases} P_{MT}(t) = \eta_{MT}\left(G_{MT}^{CH_4}(t)\,L_{CH_4} + G_{MT}^{H_2}(t)\,L_{H_2}\right) \\ H_{MT}(t) = \dfrac{P_{MT}(t)\,(1-\eta_{MT})\,\eta_{MT,re}K}{\eta_{MT}} \\ Y_{MT}^{t} = \dfrac{G_{MT}^{H_2}(t)}{G_{MT}^{H_2}(t) + G_{MT}^{CH_4}(t)} \end{cases} \tag{4}$$

In the equation: $P_{MT}(t)$ and $H_{MT}(t)$ characterize the gas turbine's dual-output energy streams (electricity and heat) at time t; $G_{MT}^{CH_4}(t)$ and $G_{MT}^{H_2}(t)$ denote the gas turbine's CH4 and H2 fuel consumption rates during operational interval t (unit: m^3); L_{CH_4} and L_{H_2} are the lower heating values (LHV) of CH_4 and H_2; η_{MT} and $\eta_{MT,re}$ define the micro gas turbine cogeneration metrics in combined heat and power operation; K is the heat production coefficient; Y_{MT}^{t} specifies the hydrogen volume fraction at time t.

The mathematical model for hydrogen-blended operation of gas-fired boilers is formulated as [27]:

$$\begin{cases} H_{GB}(t) = \eta_{GB}\left(G_{GB}^{CH_4}(t)\,H_{CH_4} + G_{GB}^{H_2}(t)\,H_{H_2}\right) \\ Y_{GB}(t) = \dfrac{\frac{G_{GB}^{H_2}(t)\rho_{H_2}}{M_{H_2}}}{\frac{G_{GB}^{H_2}(t)\,\rho_{H_2}}{M_{H_2}} + \frac{G_{GB}^{CH_4}(t)}{M_{CH_4}}\rho_{CH_4}}. \end{cases} \tag{5}$$

In the equation: $H_{GB}(t)$ is the gas-fired boiler's heat production during t; $G_{GB}^{CH_4}(t)$ and $G_{GB}^{H_2}(t)$ denote the boiler's fuel CH_4 and H_2 consumption at time t (unit:m^3) ; η_{GB} represents the gas-fired boiler 's thermal efficiency; $Y_{GB}(t)$ defines the H_2 mol fraction in the fuel blend at time t.

3.3 Carbon Emission Trading Mechanism

The carbon trading market allows participating entities to trade carbon emission allowances allocated by regulatory authorities. Market participants decide to purchase or trade emission permits depending on the gap between their measured emissions and granted caps. Regulatory authorities distribute carbon emission allowances to IES based on their previous year's total electricity generation or heat supply multiplied by a benchmark value. When an IES's CO_2 output exceeds its granted caps, acquiring additional permits from emissions trading platforms becomes necessary, generating carbon market expenses. The carbon trading market enables participating entities to buy and sell carbon emission allowances that are allocated by regulatory authorities. Participants make trading decisions, buying or selling emission permits, based on the discrepancy between their verified emissions and assigned allowances. Regulatory authorities distribute carbon emission allowances to IES based on their total electricity generation or heat supply from the previous year, multiplied by a benchmark value. An IES must buy more allowances from the carbon market when its actual emissions surpass the quota that has been allotted to it, resulting in carbon trading costs. Conversely, if an IES has surplus allowances, it can sell them to generate revenue from carbon trading. It can sell surplus allowances to generate carbon trading revenue. The carbon market framework comprises three core components: allocated emission allowances, verified CO_2 discharges, and market transaction expenses.

3.3.1 Initial Carbon Emission Allowance Allocation

At the moment, China mostly assigns initial carbon emission allowances to participants in the carbon trading market using the benchmarking approach. For an IES entirely supplied by upstream coal-fired generation, the primary carbon sources include coal-based power plants, gas-fired turbines and boilers, and gas-dependent energy demand components. The foundational carbon quota distribution framework is designed as follows [28]:

$$\begin{cases} E_{IES}^{'} = E_{th}^{'} + E_{GT}^{'} + E_{GB}^{'} + E_{GLoad}^{'} \\ E_{th}^{'} = \beta_e \sum_{t=1}^{T} P_{th}(t) \\ E_{GT}^{'} = \beta_h \sum_{t=1}^{T} \left(\varphi_{e,h} P_{MT}(t) + H_{MT}(t)\right) \\ E_{GB}^{'} = \beta_h \sum_{t=1}^{T} H_{b,t}^{GB}(t), E_{GLoad}^{'} = \beta_{GLoad} \sum_{t=1}^{T} P_{GLoad}(t) \end{cases} \tag{6}$$

In the equation: $E_{IES}^{'}, E_{e,buy}^{'}, E_{GT}^{'}, E_{GB}^{'}, E_{GLoad}^{'}$ denote the allocated CO_2 allowances for the IES, thermal power unit, gas turbine, gas boiler and gas load. β_e, β_h, β_{GLoad} denote carbon quotas allocated per unit of electricity, heat energy, and gas load consumption. $\varphi_{e,h}$ is the conversion coefficient for transforming combined heat and power (CHP) electrical output into equivalent heat output; $P_{th}(t)$ denotes the coal-based generator's electricity generation at time interval t; $P_{m,t}^{MT}$ and $H_{m,t}^{MT}$ are electrical and thermal power outputs of the gas turbine at time t; $P_{GB}(t)$ is thermal power output of the gas boiler at time t; $H_{b,t}^{GB}$ is gas-driven energy consumption at t; T is duration of a dispatch cycle.

3.3.2 Actual Carbon Emission Calculation Formula

In considering the coupling of P2G-CCS, which captures a significant amount of CO_2, along with the fact that the gas load primarily used for residential combustion still generates carbon emissions, The carbon quantification framework is defined as [28]:

$$\begin{cases} E_{IES} = E_{GT} + E_{GB} + E_{GL,oad} + E_{th} - E_{CC,a} \\ E_{th} = \sum_{t=1}^{T} \left(a_1 + b_1 P_{th}(t) + c_1 P_{th}^2(t)\right) \\ E_{GT} = \beta_h^* \sum_{t=1}^{T} \left(\varphi_{e,h} P_{MT}(t) + H_{MT}(t)\right) \\ E_{GB} = \beta_h^* \sum_{t=1}^{T} H_{GB}(t), \quad E_{GLLoad} = \beta_{GLoad}^* \sum_{t=1}^{T} P_{GLoad}(t) \\ E_{CC,a} = \sum_{t=1}^{T} E_{CC}(t) \end{cases} \tag{7}$$

In the equation: $E_{IES}, E_{e,buy}, E_{GT}, E_{GB}, E_{GL,oad}$ respectively represent the actual carbon emissions of the IES, thermal power unit, gas turbine, gas boiler, and gas load; $E_{CC,a}$ is the total carbon capture amount during the dispatch cycle; a_1, b_1 and c_1 are the actual carbon emission parameters of the coal-fired unit; β_h^* and β_{GLoad}^* are the carbon emission factor per unit thermal power output of the fired unit and carbon emission factor per unit gas load consumption; $E_{CC}(t)$ is the carbon capture amount by CCS during time interval t.

3.3.3 Tiered Carbon Trading Mechanism

Carbon trading emission rights $E_{jy}(t)$ are calculated using Eqs. (6) and (7) based on initial allowances and system emissions:

$$E_{jy}(t) = E_{IES} - E'_{IES} \tag{8}$$

To effectively incentivize deep decarbonization, this study adopts a tiered carbon trading mechanism instead of a uniform carbon price [28,29]. This mechanism imposes progressively higher carbon prices as the system's emissions exceed the allocated quota by certain intervals, creating a stronger economic signal for emission reduction.

The mechanism is activated based on the carbon emission rights $E_{jy}(t)$_trade(t) calculated as the difference between the initial allowance E_{IES} and the actual emissions E'_{IES} (Eq. (8)). The acceptance conditions are as follows:

When $E_{jy}(t) > 0$, the system has surplus allowances and can sell them in the carbon market to generate revenue, which is calculated with a compensation coefficient θ to enhance the low-carbon incentive. When $E_{jy}(t) < 0$ the system must purchase additional allowances. The tiered pricing structure is applied under this condition, where the cost increases stepwise as the absolute value of $E_{jy}(t) < 0$ falls into higher intervals.

The limits of this mechanism are defined by its key parameters in the cost calculation model (Eq. (9)), which are set with reference to existing policy designs and academic research [22,28]:

$$f_{CO_2}(t) = \begin{cases} -\chi(2+3\delta)L + \chi(1+3\delta)\left(E_{jy}^t + 2L\right), \\ E_{jy}^t \le -2L \\ -\chi(1+\delta)L + \chi(1+2\delta)\left(E_{jy}^t + L\right), \\ -2L < E_{jy}^t \le -L \\ \chi(1+\delta)E_{jy}^t, -L < E_{jy}^t \le 0 \\ \chi E_{jy}^t, 0 < E_{jy}^t \le L \\ \chi L + \chi(1+\theta)\left(E_{jy}^t - L\right), \\ L < E_{jy}^t \le 2L \\ \chi(2+\theta)L + \chi(1+2\theta)\left(E_{jy}^t - 2L\right) \\ 2L \le E_{jy}^t \end{cases} \tag{9}$$

In the equation: χ is reference allowance pricing baseline; L is the carbon-emitting period length; θ is the carbon cost escalation speed; δ is the compensation coefficient; $f_{CO_2}(t)$ is the System's carbon trading cost at time t, positive value indicates allowance purchase, negative value indicates allowance sale.

3.4 Modeling Additional System Elements

3.4.1 Electric Resistance Boiler

$$H_{EB}(t) = \eta_{EB} P_{EB}(t) \tag{10}$$

In the equation: $H_{EB}(t)$ represents the heat generation from the electric resistance boiler (ERB) in time interval t; $P_{EB}(t)$ denotes the electrical power supplied to the ERB during period t; η_{EB} corresponds to the ERB's efficiency in converting electrical energy to thermal energy.

3.4.2 Energy Storage System

$$\begin{cases} W_{ES}(t+1) = W_{ES}(t)\left(1-\sigma^{ES}\right) + \left(P_{ES}^{chr}(t)\,\eta^{ES,chr} - \dfrac{P_{ES}^{dis}(t)}{\eta^{ES,dis}}\right) \\ W_{HS}(t+1) = W_{HS}(t)\left(1-\sigma^{HS}\right) + \left(H_{HS}^{chr}(t)\,\eta^{HS,chr} - \dfrac{H_{HS}^{dis}(t)}{\eta^{HS,dis}}\right) \end{cases} \tag{11}$$

In the equation: $W_{ES}(t)$ is the stored electrical energy capacity at time t; $W_{HS}(t)$ is the stored thermal energy capacity at time t; σ^{ES} and σ^{HS} are the electrical storage self-dissipation rate and thermal storage self-dissipation rate; $P_{ES}^{chr}(t)$ and $P_{ES}^{dis}(t)$ are the energy storage charge-discharge capacity during t ; $H_{HS}^{chr}(t)$ and $H_{HS}^{dis}(t)$ are the thermal storage energy charge-discharge at t; $\eta^{ES,chr}$ and $\eta^{ES,dis}$ are the energy storage charge/discharge efficiency; $\eta^{HS,chr}$ and $\eta^{HS,dis}$ are the thermal storage charge/discharge efficiency.

3.5 Optimal Dispatch Strategy

3.5.1 Operational Objective

An ideal dispatch model is created for an IES that integrates P2G with CCS and hydrogen-blended natural gas in order to reduce the overall operating cost F while striking a balance between environmental sustainability and economic performance.

$$\min F = F_{CO_2} + F_f + F_{th1} + F_{th2} + F_{buy}^{g} + F_{cur} \tag{12}$$

In the equation: F denotes the overall operational expenditure of the system; F_{CO_2} corresponds to the expenses associated with carbon trading; F_f denotes the carbon sequestration cost; F_{th1} represents the start-up and shutdown expenditure of coal-fired units; F_{th2} is the coal consumption cost; F_{buy} is the gas procurement cost; F_{cur} is the wind curtailment cost.

After implementing CCS, the energy consumption required for CO_2 capture increases significantly. This energy could otherwise meet demand-side load requirements and generate electricity sales revenue. The cost of carbon capture incorporates missed revenue from forgone power generation sales. Carbon sequestration involves expenditures on compression, transport, and storage. The mathematical expressions for carbon trading and carbon capture costs are defined as follows:

$$F_{CO_2} = \sum_{t=1}^{T}\left(f_{CO_2}(t)\right) \tag{13}$$

$$F_f = \sum_{t=1}^{T}\left(c_f E_{storage}(t)\right) \tag{14}$$

In the formula: c_f is the cost of sequestering per unit mass of CO_2; $E_{storage}(t)$ is the CO_2 storage level at t; T is the duration of the dispatch cycle.

The following are the precise formulas for coal-fired units' start-up/shutdown and coal consumption costs:

$$F_{th1} = S\sum_{t=2}^{T}\left(v_{th}(t)\left(1-v_{th}(t-1)\right) + v_{th}(t-1)\left(1-v_{th}(t)\right)\right) \tag{15}$$

$$F_{th2} = \sum\left(a_1\left(P_{th}(t)\right)^2 + b_1 P_{th}(t) + c_1\right) \tag{16}$$

In the equation: S denotes the start-stop cost coefficient of the coal-fired unit; $v_{th}(t)$ serves as a binary variable indicating the operational status of the unit at time t; a_{1th}, b_{1th} and c_{1th} represent the coal-fired unit's cost coefficients for coal consumption.

The following is the term for the wind curtailment cost:

$$F_{cur} = \lambda_{cur} \sum_{t=1}^{T} P_{cur}(t) \tag{17}$$

In the equation: $P_{cur}(t)$ represents the curtailed wind power during time period t; λ_{cur} denotes the penalty cost per unit of curtailed wind power.

The expression for gas procurement cost is as follows:

$$F_{buy}^{g} = \sum_{t=1}^{T} \left(c_{buy} Q_{buy}(t) \right) \tag{18}$$

In the equation: c_{buy} is the natural gas price; $Q_{buy}(t)$ denotes the equivalent power value of the natural gas acquired by the system at time t.

3.5.2 Constraints

1) Without considering IES saling electricity from the upstream grid, the electrical power balance constraint is:

$$\begin{cases} P_{MT}(t) + P_{th}(t) + P_{Wind}(t) + P_{ES}^{dis}(t) = P_{EB}(t) + P_{P2G}^{e}(t) + P_{CCS}(t) + P_{Load}(t) + P_{ES}^{chr}(t) \\ 0 \leqslant P_{e,buy}(t) \leqslant P_{e,buy}^{\max}, 0 \leqslant P_{Wind}(t) \leqslant P_{Wind}^{\max} \end{cases} \tag{19}$$

In the formula: $P_{Wind}(t)$ is the wind turbine power supply at time t; $P_{Load}(t)$ reflects the load-side power demand at time t; $P_{e,buy}^{\max}$ is the power purchase upper limit; $P_{Wind}^{\max}$ is the maximum wind turbine output.

2) Heat power balance constraint

$$H_{MT}(t) + H_{EB}(t) + H_{HS}^{dis}(t) + H_{GB}(t) = H_{Load} + H_{HS}^{chr}(t) \tag{20}$$

In the formula: $H_{Load}(t)$ reflects the corresponds to the heat load requirement at t; $H_{HS}^{dis}(t)$ and $H_{HS}^{chr}(t)$ define the discharging/charging capacity of the heat storage unit during period t.

3) Limitationon gas power balance

$$Q_{Load}(t) + G_{MT}^{CH_4}(t) + Q_{GB}^{CH_4}(t) = Q_{H_{2G,out}}(t) + Q_{buy}(t) \tag{21}$$

In the formula: $Q_{H_{2G,out}}(t)$ corresponds to the methanation-generated gas output at time t; $Q_{buy}(t)$ indicates the system's gas procurement rate during operation.

4) Limitation on hydrogen power balance

$$G_{MT}^{H_2}(t) + G_{GB}^{H_2}(t) + Q_{H2G,in}(t) = P_{P2g}^{H_2}(t) \tag{22}$$

In the formula: $Q_{H2G,in}(t)$ denotes the hydrogen power consumption during the methanation process; $P_{P2g}^{H_2}(t)$ is the denotes the H2 output rate of the P2G unit during period t;

5) Wind power output constraints

$$\begin{cases} P_{WT}(t) = P_{cur}(t) + P_{Wind}(t) \\ 0 \le P_{Wind}(t) \le P_{WT}(t) \end{cases} \tag{23}$$

In the equation: $P_{WT}(t)$ corresponds to the forecasted wind generation during period t; $P_{cur}(t)$ indicates the system's wind energy curtailment level at time t.

6) Gas turbine output constraints

$$\begin{cases} P_{MT}^{\min} \le P_{MT}(t) \le P_{MT}^{\max} \\ H_{MT}^{\min} \le H_{MT}(t) \le H_{MT}^{\max} \\ \Delta Q_{MT}^{\min} \le Q_{MT}(t) - Q_{MT}(t-1) \le \Delta Q_{CHP}^{\max} \end{cases} \tag{24}$$

In the formula: $P_{MT}^{\min}$ and $P_{MT}^{\max}$ denote the gas turbine's electrical generation capacity thresholds; $H_{MT}^{\min}$ and $H_{MT}^{\max}$ denote the gas turbine's thermal generation capacity thresholds; $\Delta Q_{MT}^{\min}$ and $\Delta Q_{CHP}^{\max}$ characterize the gas turbine's operational ramp constraint.

7) Gas boiler output constraints

$$\begin{cases} H_{GB}^{\min} \le H_{GB}(t) \le H_{GB}^{\max} \\ \Delta H_{GB}^{\min} \le H_{GB}(t) - H_{GB}(t-1) \le \Delta H_{GB}^{\max} \end{cases} \tag{25}$$

In the formula: $H_{GB}^{\min}$ and $H_{GB}^{\max}$ indicate the lowest and highest heat generation of the gas boiler; $\Delta H_{GB}^{\min}$ and $\Delta H_{GB}^{\max}$ are the ramp rate upper and lower limits of the gas boiler.

8) Thermal power unit output constraints

$$\begin{cases} P_{th}^{\min} \le P_{th}(t) \le P_{th}^{\max} \\ \Delta P_{th}^{down} \le P_{th}(t) - P_{th}(t-1) \le \Delta P_{th}^{up} \end{cases} \tag{26}$$

In the formula: $P_{th}^{\min}$ and $P_{th}^{\max}$ denote the gas turbine's thermal generation capacity thresholds; ΔP_{th}^{down} and ΔP_{th}^{up} define the upper and lower ramping rate boundaries for thermal generators.

9) Energy storage constraints

Electrical and thermal storage systems share equivalent operating limits. Therefore, only the EES constraints are explicitly defined here; the TES constraints follow the same principle as follows:

$$\begin{cases} W_{ES}^{\min} \le W_{ES}(t) \le W_{ES}^{\max} \\ W_{ES}^{0} = W_{ES}^{T} \\ 0 \le P_{ES}^{chr}(t) \le \chi_{ES}^{chr} P_{ES}^{chr,\max} \\ 0 \le P_{ES}^{dis}(t) \le \chi_{ES}^{dis} P_{ES}^{dis,\max} \\ 0 \le \chi_{ES}^{dis} + \chi_{ES}^{chr} \le 1 \end{cases} \tag{27}$$

In the formula: $W_{ES}^{\min}$ and $W_{ES}^{\max}$ are the lower and upper operational limits of the storage unit; W_{ES}^{0} and W_{ES}^{T} represent the initial and final values during the operational cycle; χ_{ES}^{dis} and χ_{ES}^{chr} are the discharging and charging state at time t; $P_{ES}^{chr,\max}$ and $P_{ES}^{dis,\max}$ indicate the peak permissible charging/discharging power thresholds for the system during time interval t.

10) CCS device constraints

$$\begin{cases} 0 \le P_{CCS}(t) \le P_{CCS}^{\max} \\ 0 \le V_{CO_2}(t) \le V_{CO_2}^{\max} \end{cases} \tag{28}$$

In the formula: $P_{CCS}^{\max}$ defines the rated maximum electrical power consumption threshold of the CCS system; $V_{CO_2}^{\max}$ is the maximum carbon dioxide supply limit for the carbon capture equipment.

11) P2G output constraints

$$\begin{cases} P_{P2G}^{e,\min} \le P_{P2G}^{e}(t) \le P_{P2G}^{e,\max} \\ \Delta P_{P2G}^{e,down} \le P_{P2G}^{e}(t) - P_{P2G}^{e}(t-1) \le \Delta P_{P2G}^{e,up} \end{cases} \tag{29}$$

In the formula: $P_{P2G}^{e,\min}$ and $P_{P2G}^{e,\max}$ are the minimum and maximum electrolytic power consumption limits; $\Delta P_{P2G}^{e,down}$ and $\Delta P_{P2G}^{e,up}$ define the upward and downward ramping rate operational boundaries for the power-to-gas conversion unit.

12) Electric heating boiler output constraints

$$\begin{cases} H_{EB}^{\min} \le H_{EB}(t) \le H_{EB}^{\max} \\ \Delta H_{EB}^{down} \le H_{EB}(t) - H_{EB}(t-1) \le \Delta H_{EB}^{up} \end{cases} \tag{30}$$

In the formula: $H_{EB}^{\max}$ and $H_{EB}^{\min}$ specify the operational heat generation range of the electric boiler; ΔH_{EB}^{down} and ΔH_{EB}^{up} are the ramping constraints of the electric heating boiler.

3.6 Model Linearization

The integrated energy system scheduling model incorporating P2G-CCS coupling and hydrogen-blended natural gas under tiered carbon trading, established in this paper, is a Mixed-Integer Nonlinear Programming (MINLP) model. Consequently, it must be transformed into a Mixed-Integer Linear Programming (MILP) model to be solved using CPLEX. Eq. (9) is linearized by introducing binary (0–1) variables, while Eq. (15) is linearized using the Big-M method. When optimizing the time-varying hydrogen blending ratio, the model becomes more complex. Therefore, a hybrid solution strategy is adopted, which employs the Particle Swarm Optimization (PSO) algorithm to call the CPLEX solver. The specific flowchart is illustrated in Fig. 3. In this framework, the position of each particle in the PSO represents the 24-h hydrogen blending ratios for the gas turbine and gas boiler, and the fitness function is encapsulated by the optimal scheduling program.

4 Case Analysis

4.1 Case Parameters

The IES in this paper comprises a wind power plant, gas-fired boilers, gas turbines, hydrogen-producing P2G devices, CCS devices, electric heating boilers, thermal energy storage, electrical energy storage devices, and coal-fired power units. The parameters of all devices are listed in Table 1, while the electrical/thermal loads and wind power forecast are shown in Fig. 4.

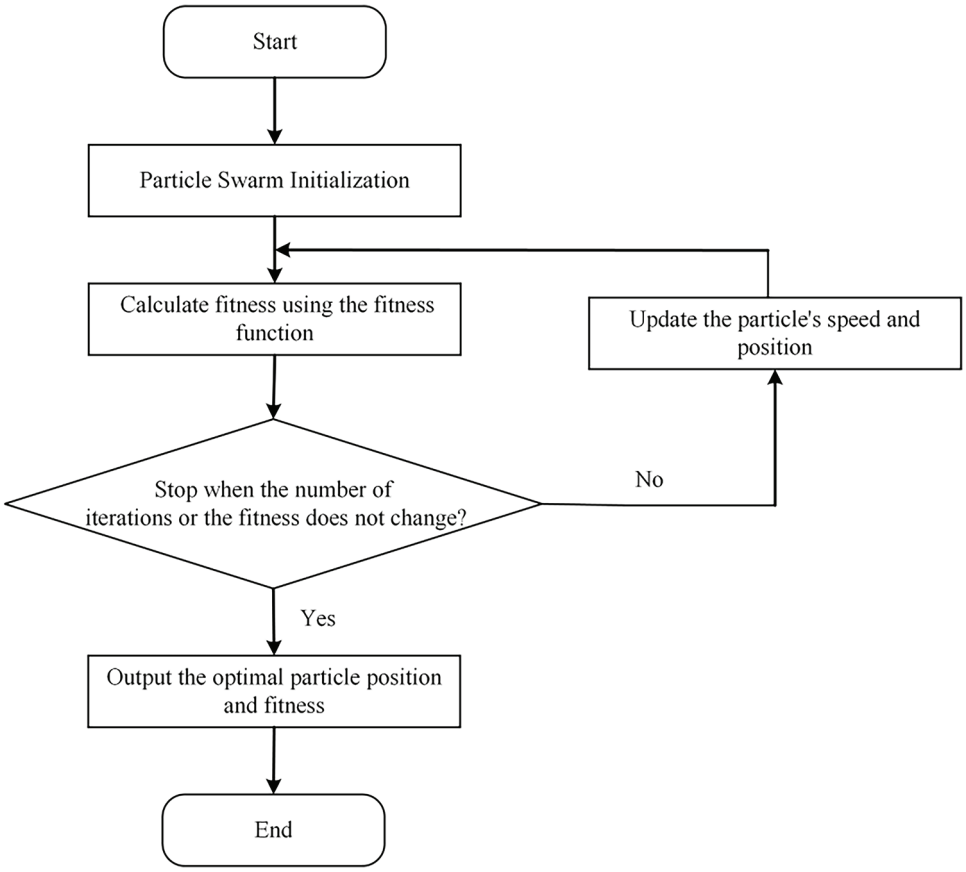

Figure 3: Solving process of particle swarm optimization combined with YAMILP

Table 1: Parameters of each device

Equipment	Parameter	Value
Gas turbine	Maximum/minimum generation power/MW	350/0
	Maximum/minimum heat production power/MW	300/0
	Total power ramping up/down limits/(MW/h)	150/−150
	Heat production efficiency/Power generation efficiency	0.4/0.35
Gas boiler	Peak/base thermal generation thresholds/MW	80/0
	Heat production power ramping up/down limits/(MW/h)	25/−25
	Conversion efficiency	0.92
Electric heating boiler	Maximum/minimum power consumption/MW	40/0
	Power consumption ramping up/down limits/(MW/h)	10/−10
	Electric-heat conversion efficiency	0.9

(Continued)

Table 1 (continued)

Equipment	Parameter	Value
Thermal power unit	Peak/base load demand thresholds/MW	162/45
	Output ramping up/down limits/(MW/h)	100/−100
P2G	Electrohydrogen conversion efficiency	0.85
	Methanation efficiency	0.7
	Maximum/minimum power consumption/MW	120/0
	Maximum operating condition energy consumption/MW	150
CCS	Rich solution storage device max/min capacity/m^3	29,200/0
	Lean solution storage device max/min capacity/m^3	29,200/0
	Initial capacity of rich/lean solution storage/m^3	14,600/14,600
Heat storage	Thermal energy storage boundary conditions/(MW/h)	120/20
	Maximum charge/discharge power/MW	15/15
	Charge/discharge efficiency	0.95/0.95
	Heat loss coefficient	0.01
	Starting storage level/(MW·h)	60
Energy storage	Electricity storage capacity upper/lower limit/(MW·h)	60/10
	Maximum charge/discharge power/MW	5/5
	Charge/discharge efficiency	0.9/0.9
	Self-discharge coefficient	0.001
	Starting storage level/(MW·h)	30

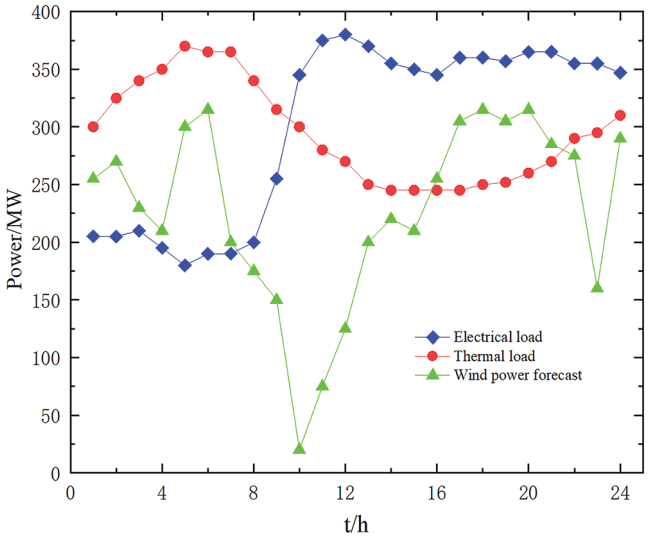

Figure 4: Electro-thermal load and wind power forecasted output

4.2 Analysis of the P2G-CCS Coupling Model

This research establishes three simulation scenario to evaluate how the integration of P2G-CCS influences both environmental sustainability and cost-effectiveness in IES. Scenario 1 considers the P2G-CCS coupling. Scenario 2 incorporates the P2G-CCS coupling but excludes methanation, with hydrogen production solely used for hydrogen blending in gas-fired equipment; gas turbines and gas boilers maintain a fixed hydrogen blending ratio of 10%. Scenario 3 does not consider CCS, where emitted CO_2 is directly released into the atmosphere, and CO_2 for methanation is purchased externally for 2.8 CNY/m^3. All three scenarios adopt a fixed hydrogen blending ratio of 10%. The following are the parameters for carbon trading: base price of 215 CNY/t, compensation coefficient of 0.25, interval length L = 50 t, and carbon price growth rate of 25%.

The outcomes of the three scenarios' optimum scheduling are displayed in Table 2. Compared to Scenario 2, Scenario 1 has an 11.8% lower total cost but a 23.6% higher coal consumption cost and a 196,530 CNY reduction in wind curtailment cost. This is because Scenario 1 includes an additional methanation process, which increases the electricity consumption for hydrogen feedstock production, thereby raising the output of coal-fired units and enhancing wind power utilization. Due to the P2G-CCS coupling reducing gas procurement through methanation, Scenario 1's gas procurement cost is 267,570 CNY lower than Scenario 2. Regarding system carbon emissions, Scenario 1 emits 13.736 t more CO_2 than Scenario 2 under P2G-CCS coupling. This indicates that while methanation increases energy consumption (leading to higher coal-fired unit output and carbon emissions), it reduces gas procurement costs, enhances the low-carbon economic benefits of hydrogen-blended gas turbines, and improves renewable energy utilization for hydrogen production, effectively absorbing curtailed wind power. Scenario 3, which does not consider carbon capture, sees its total cost increase from 4,071,750 CNY to 6,487,320 CNY, with a daily operating cost increase of 2,415,570 CNY, rise of 59.3% compared to Scenario 1. This is due to the need to purchase large carbon quotas for direct CO_2 emissions into the atmosphere. The findings in Table 1 show that P2G-CCS coupling can increase the system's rate of renewable energy usage while lowering IES carbon emissions and overall operating expenses.

Table 2: Optimal dispatch results for scenarios 1–3

Scenario	Scenario 1	Scenario 2	Scenario 3
Total cost (10^4 CNY)	407.175	455.319	648.732
Gas procurement cost (10^4 CNY)	412.175	438.932	413.75
Carbon trading cost (10^4 CNY)	−111.580	−104.929	132.764
Coal consumption cost (10^4CNY)	16.155	13.063	17.880
Wind curtailment cost (10^4 CNY)	38.002	57.655	38.014
Carbon purchase cost (10^4 CNY)	0	0	16.324
Carbon sequestration cost (10^4 CNY)	37.327	35.598	0
Startup/Shutdown cost (10^4 CNY)	15	15	30
Carbon Emissions/t	2920.107	2907.843	6226.414

4.3 Analysis of Hydrogen Blending in the System

4.3.1 Analysis of the Advantages of Fixed Hydrogen Blending in Gas Boilers and Turbine

Scenario 4 (non-hydrogen blending) and Scenario 5 (variable hydrogen blending ratio) were established as comparative cases based on Scenario 1 to validate the low-carbon characteristics and economic

viability. Tables 3 and 4, respectively, present the post-optimization energy production/consumption of equipment, dispatch costs, and carbon emission profiles for these two scenarios.

Table 3: Energy production and consumption of various devices after optimization in different hydrogen blending scenarios

Scenario	Scenario 1	Scenario 2	Scenario 5
Coal-fired power output (MW·h)	1228.989	1246.094	1182.046
Gas turbine thermal output (MW·h)	4530.679	4353.724	4330.690
Gas turbine electrical output (MW·h)	4189.344	3809.508	3789.354
Electric boiler energy consumption (MW·h)	940.839	920.000	934.125
Gas boiler energy consumption (MW·h)	1913.143	1910.486	1920.000
Carbon capture energy consumption (MW)	113.512	177.285	110.39
Electrolysis energy consumption (MW·h)	1564.115	1099.554	1236.591

Table 4: Carbon emissions and dispatch costs under various hydrogen mixing scenarios

Scenario	Scenario 1	Scenario 4	Scenario 5
Total cost (10^4 CNY)	407.175	429.02	394.758
Gas procurement cost (10^4 CNY)	412.175	419.279	410.050
Carbon trading cost (10^4 CNY)	−111.580	−101.553	−117.475
Coal consumption cost (10^4 CNY)	16.155	20.435	19.385
Wind curtailment cost (10^4 CNY)	38.002	38.000	31.426
Carbon sequestration cost (10^4 CNY)	37.327	37.327	36.372
Startup/Shutdown cost (10^4 CNY)	15	15	15
Total carbon emissions (ton)	3229.085	3443.385	3277.075

As shown in Table 3, the coal-fired unit output in Scenario 1 remains nearly unchanged compared to Scenario 4, while the gas turbine power output increases. This is due to the increased hydrogen demand in Scenario 1 with hydrogen blending, which raises the system's electrolysis output, thereby enhancing the production of hydrogen-blended gas turbines with lower carbon emissions. Although the gas turbine output increases, the CO_2 emissions per unit output decrease. Additionally, owing to the thermoelectric coupling effect of gas turbines and fixed heat load demand, gas turbines' increased thermal output reduces gas boilers' thermal output. Furthermore, gas boilers operating with hydrogen blending further reduce CO_2 emissions. Consequently, Scenario 1 achieves a 114.3 t reduction in carbon emissions compared to Scenario 4.

As shown in Table 4, the total operating cost in Scenario 5 decreases by 2.8% and 4.6% compared to Scenarios 1 and 4, respectively, primarily due to higher carbon trading revenue and lower wind curtailment costs. Additionally, Scenario 5 reduces carbon emissions by 52.10 t and 166.31 t relative to Scenarios 1 and 4, demonstrating that appropriate hydrogen blending ratios can effectively enhance system decarbonization. Although the variable hydrogen blending ratio incurs additional carbon sequestration costs, its electrolysis and carbon capture energy consumption are the lowest among the three scenarios, indicating higher energy utilization efficiency.

In summary, blending hydrogen into gas turbines and boilers decreases carbon emissions in the system while expanding carbon quota allocations, which enhances revenue from carbon trading and ultimately reduces total system-wide emissions.

4.3.2 Comparative Analysis of Hydrogen Blending Benefits under Different Blending Ratios

The effect of hydrogen blending ratios on overall operating expenses and CO_2 emissions is examined in this section. Figs. 5 and 6 present the cost and emission curves under varying hydrogen blending ratios, with 2%, 6%, 10%, 14%, and 18% representing the hydrogen blending ratios applied to gas boilers.

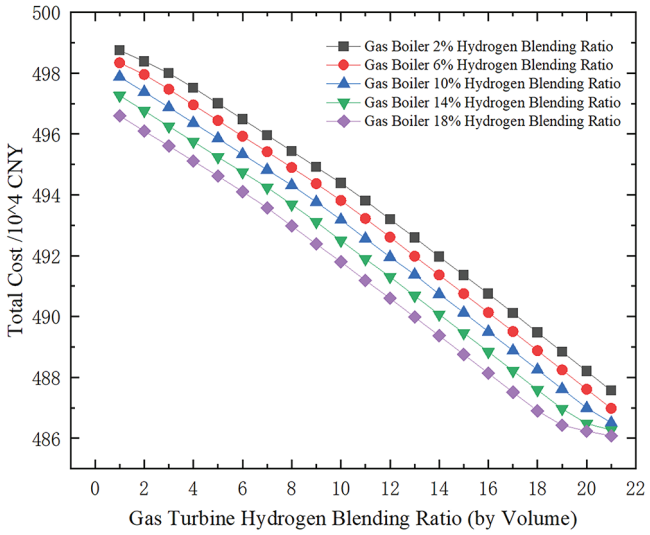

Figure 5: System total costs under different hydrogen blending ratios

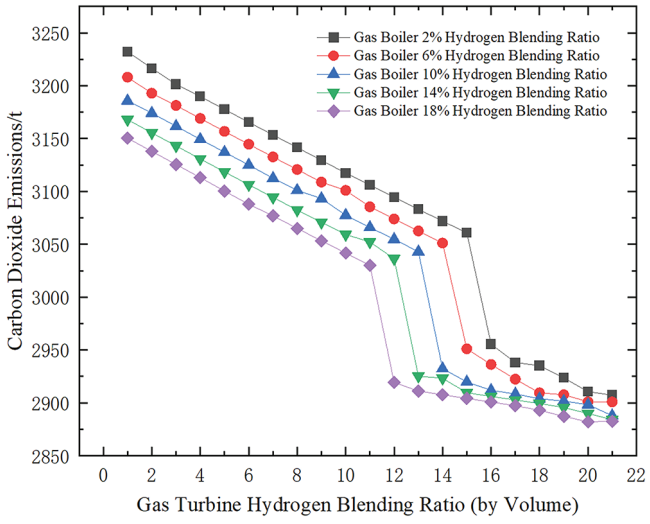

Figure 6: Carbon emissions under different hydrogen blending ratios

Fig. 5 reveals that system costs progressively decline with higher hydrogen blending ratios, but the rate of reduction diminishes as ratios increase. When the hydrogen blending ratio for gas boilers reaches 18%, the total cost trend becomes progressively flatter at an 18% hydrogen blending ratio for gas turbines. Fig. 6

indicates that CO_2 emissions decline with higher blending ratios. After the gas boiler blending ratio exceeds 18% and the gas turbine blending ratio surpasses 12%, the CO_2 reduction trend stabilizes, and the overall emission curve levels off. The differences in total costs and carbon emissions across varying gas boiler blending ratios decrease as the gas turbine blending ratio rises

This analysis demonstrates that, from both emission reduction and economic perspectives, when the gas boiler hydrogen blending ratio is fixed at 18%, the total cost decreases minimally once the gas turbine blending ratio exceeds 18%, while CO_2 emissions plateau after the gas turbine blending ratio reaches 12%. Therefore, a reasonable configuration of hydrogen blending ratios for gas turbines and boilers can reduce system emissions without significantly increasing operational costs.

4.3.3 Benefit Analysis of Optimized Hydrogen Blending Ratios

Under fixed hydrogen blending ratio operation, gas boilers and gas turbines require electrolysis to produce hydrogen, leading to mandatory electrolysis output that increases unit operation. This issue can be resolved by adopting time-varying blending ratios.

Tables 2 and 3 show the optimization results with variable hydrogen blending ratios. Compared to fixed ratios, the variable strategy reduces carbon trading costs by 84,700 CNY, total system costs by 132,500 CNY, gas purchasing costs by 21,250 CNY, and carbon emissions by 52.01 t. This indicates that variable hydrogen blending ratios reduce gas turbine output and lower fuel costs and emissions.

Fig. 7a illustrates the hydrogen power consumption of gas turbines and boilers, Fig. 7b illustrates the net load profiles under fixed and variable blending modes. The variable strategy consumes less hydrogen load than the fixed mode. Reducing hydrogen blending during high net load periods decreases mandatory turbine output. Calculations from Tables 2 and 3 show a 599.979 MWh reduction in total turbine output, a 6.88% decrease, and a 327.594 MWh reduction in electrolysis power consumption, a 20.93% efficiency improvement. These results demonstrate that optimizing hydrogen blending ratios for gas turbines and boilers can effectively reduce system operational loads and energy consumption.

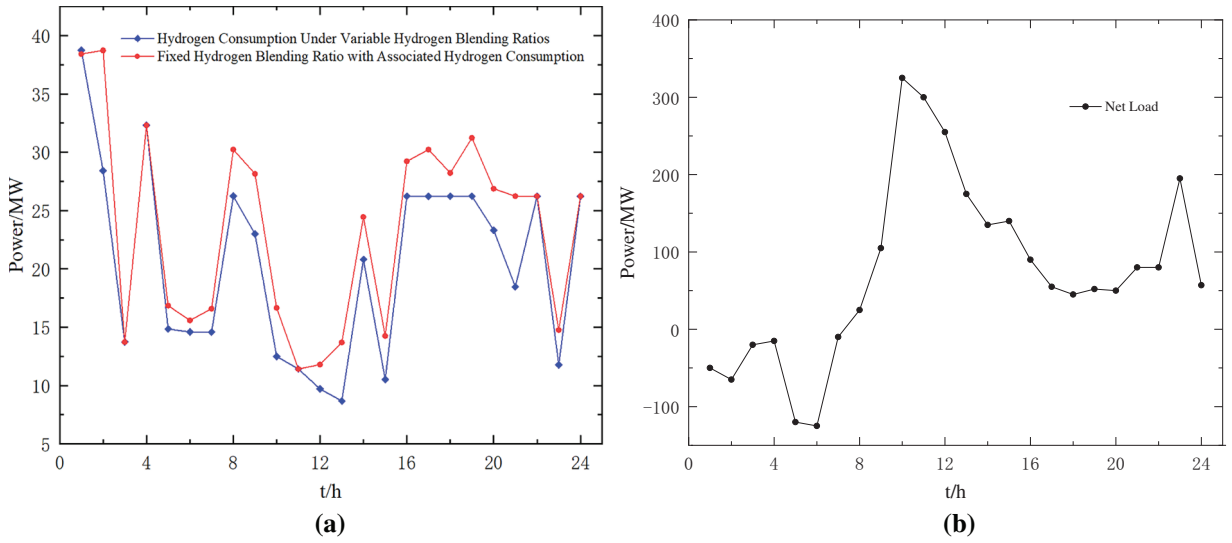

Figure 7: Hydrogen consumption-power correlation and net load profiles

4.3.4 Hydrogen Analysis for Each Period of the System

Fig. 8 below gives the hydrogen balance results for each period, as shown in the figure, the peak output of wind power is 0:00–08:00, the output of renewable energy is high, and the power demand of the gas turbine is low, the gas boiler only meets the basic heating demand, and the consumption of electricity by the gas turbine is small, so the system starts methanation, converts hydrogen into methane for storage, and the gas turbine and gas boiler also maintain hydrogen doping operation, reducing the operating cost of the system, and in the 08:00–18:00 period, In this period, due to the high energy demand of the system, the output of the gas turbine and the gas boiler is high, so the hydrogen production of the system in this period is not enough for methanation, so the methanation process is not carried out. Between 18:00 and 24:00, the production of hydrogen for methanation and gas blending is increased due to the decrease in electricity demand and the increase in wind power output. Multi-hydrogen utilization can diversify the hydrogen generated during the water electrolysis process in P2G, reducing energy discarding and increasing the uptake of renewable energy.

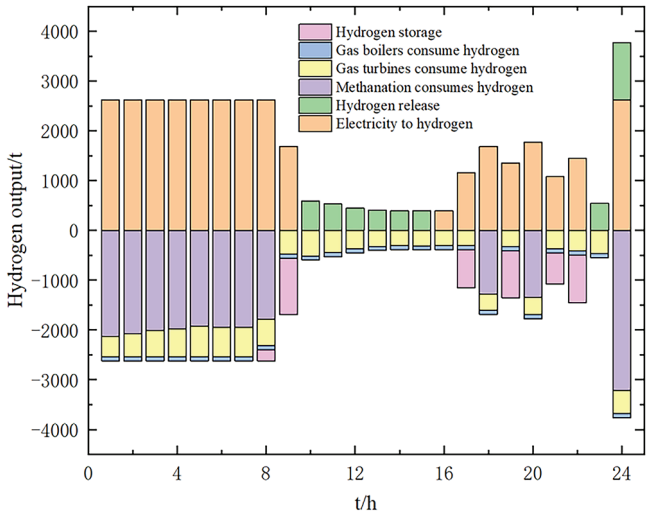

Figure 8: Hydrogen equilibrium results of the system

Fig. 9 shows the specific direction of hydrogen generation and consumption of the system, where in the process of hydrogen generation, The power-to-hydrogen device produced 34.188 t of hydrogen, the hydrogen storage tank released 4.455 t of hydrogen, in the hydrogen consumption process, the hydrogen storage tank stored 4.639 t of hydrogen, the gas boiler consumed 1.999 t of hydrogen, the gas turbine consumed 10.349 t of hydrogen, and the methanation consumed 21.654 t of hydrogen, as can be seen from the figure, the hydrogen of the power-to-hydrogen device is mainly supplied to the methanation process of the system, and also to the gas unit, as can be seen from Table 2, when the system considers methanation, the system cost is reduced by 481,440 CNY compared with not considering methanation This is mainly due to the reduction of the gas purchase cost and curtailment cost of the system through methanation, and because the hydrogen doping of the gas unit is considered, it can be seen from Table 4 that the carbon emission of the system is reduced by 114.3 t compared with the non-hydrogen doping. Therefore, it can be seen that methanation and gas hydrogen blending reduce the total cost and carbon emissions of the system, and increase the absorption rate of renewable energy.

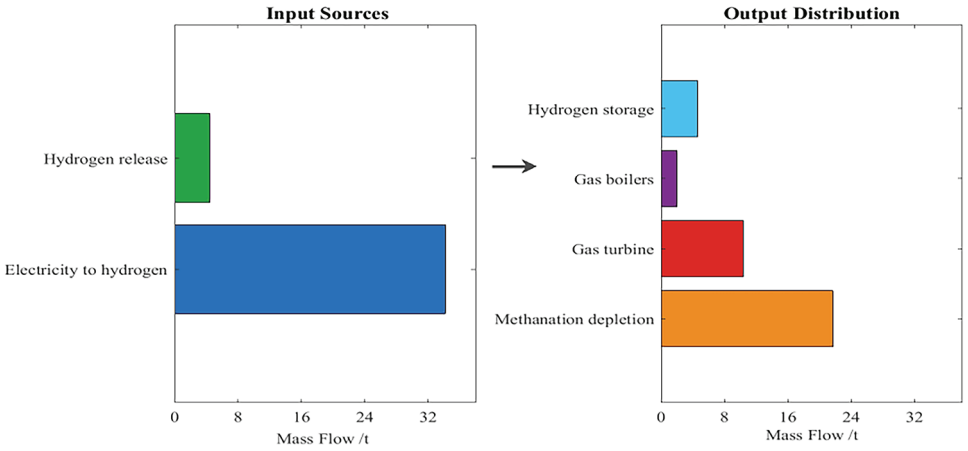

Figure 9: Hydrogen generation and output of the system

4.3.5 Economic Performance and Trade-Off Analysis

While the proposed strategy effectively reduces the total operational cost and carbon emissions, it relies on the deployment and operation of key infrastructures like P2G and CCS, introducing inherent trade-offs. The introduction of the P2G-CCS coupling system and hydrogen-blending infrastructure increases capital investment and operational energy consumption. However, these investments are offset through multiple pathways:

Reduced Fuel Costs: Synthetic natural gas produced by P2G directly substitutes purchased natural gas, while hydrogen blending reduces natural gas consumption per unit of energy output. Scenario 1 has a gas purchase cost reduction of 267,570 CNY compared to scenario 2.

Increased Carbon Trading Revenue/Reduced Expenditure: CCS significantly reduces the system's net carbon emissions, allowing the system to sell substantial surplus allowances in the tiered carbon market, generating significant income.Scenario 1 has a carbon trading cost reduction of 2,443,440 CNY compared to Scenario 3.

Lower Wind Curtailment Penalties: P2G consumes curtailed wind power, converting penalty costs into valuable energy products. Scenario 1, compared to Scenario 3, reduces the cost of wind abandonment by 196,530 CNY.

The case study results demonstrate that although Scenario 1 incurs higher carbon capture energy consumption and coal consumption costs due to operating P2G-CCS (see Table 2), its substantial advantages in carbon trading revenue and gas procurement cost savings completely outweigh these additional costs, ultimately achieving the lowest total cost. This indicates that, under the current carbon and natural gas price regimes, investing in P2G-CCS and hydrogen blending technologies is economically viable from a full life-cycle operational perspective for the described IES.

4.4 Analysis of Tiered Carbon Trading Mechanisms

4.4.1 Benefit Analysis of Tiered Carbon Trading Mechanism

To analyze the efficacy of the tiered carbon trading framework, three operational modes are defined under a fixed 10% hydrogen blending ratio: Scenario 1 adopts the tiered carbon pricing system, Scenario 6 utilizes a flat-rate carbon trading policy, and Scenario 7 excludes carbon trading entirely. This methodology

enables systematic quantification of distinct carbon pricing strategies' effects on system economics and emission performance.

According to Table 5, the tiered carbon trading mechanism decreased overall system operating costs by 5.64% when compared to scenarios without carbon trading and 7.69% when compared to the uniform carbon trading strategy. Carbon emissions decreased by 256.801 t and 5661.42 t relative to Scenario 6 and Scenario 7. This highlights the dual benefits of integrating the tiered carbon trading framework with carbon capture technology in lowering both operational expenditures and carbon footprints. While the uniform carbon trading mechanism achieves emission reductions, dispatch outcomes in Table 4 reveal that Scenario 6 incurs higher total costs than Scenario 7. This cost disparity stems from increased energy consumption induced by carbon capture adoption, which escalates coal-fired generation costs, gas procurement expenses, and carbon sequestration expenditures.

Table 5: Optimized dispatch costs and carbon emissions under different carbon trading mechanisms

Scenario	Scenario 1	Scenario 6	Scenario 7
Total cost (10^4 CNY)	407.175	438.527	430.161
Gas procurement cost (10^4CNY)	412.175	390.466	329.516
Carbon trading cost (10^4 CNY)	−111.580	−78.689	0.000
Coal consumption cost (10^4 CNY)	16.155	31.204	32.048
Wind curtailment cost (10^4 CNY)	38.002	45.667	40.660
Carbon sequestration cost (10^4 CNY)	37.327	34.879	8.098
Startup/Shutdown cost (10^4 CNY)	15	15	15
Total carbon emissions (ton)	3329.085	3485.886	8890.505

4.4.2 Analysis of Tiered Carbon Trading Parameters

Fig. 10 illustrates the impact of carbon trading base prices on total costs and carbon emissions. Fig. 10a,b illustrates the impact of the base carbon trading price on total cost and carbon emissions under the tiered carbon trading mechanism and the unified carbon trading mechanism, respectively. For the tiered carbon trading mechanism, when the price is below 150 CNY, the system's carbon emissions gradually decrease as the base price increases. However, Carbon emissions plateau once expenditures surpass 150 CNY. This phenomenon occurs because higher prices increase the revenue generated from selling each unit of carbon emission allowance, incentivizing entities to reduce CO_2 emissions to maximize tradable allowances.

In contrast, under the uniform carbon trading mechanism, carbon emissions only stabilize when the price reaches 210 CNY, demonstrating that the tiered mechanism imposes stricter emissions constraints. Regarding total costs, the tiered mechanism achieves a total cost reduction of 4,778,530 CNY at a base price of 300 CNY, whereas the uniform mechanism only reduces costs to 4,801,250 CNY under the same price level. The tiered carbon trading mechanism's greater economic efficiency for systems with carbon capture units is further supported by this comparison.

With a base carbon price of 120 CNY, Fig. 11 shows how price increase rates affect total costs and atmospheric CO_2 levels. The price growth rate mechanism only occurs when actual carbon emissions exceed allocated quotas. The total system cost gradually rises as the price growth rate increases while CO_2 emissions progressively decline. This happens because exceeding the defined interval length triggers higher carbon trading prices, incentivizing operational adjustments to reduce emissions and lower carbon trading costs by optimizing the output distribution of system equipment and modifying emission patterns. When the price

growth rate surpasses 0.45, the increase in total expenses gradually slows down, indicating the need for coordinated adjustments in the base carbon price to maintain system efficiency.

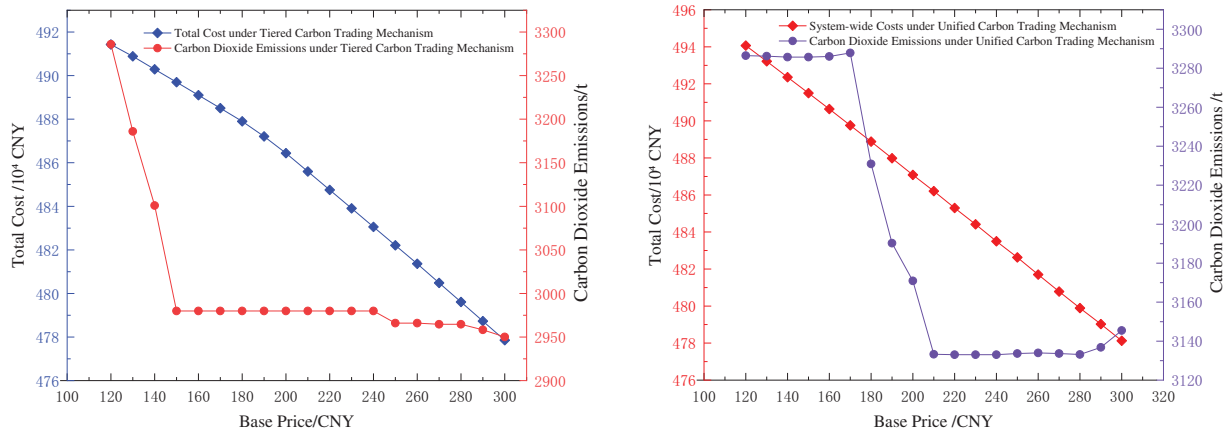

(a) Tiered Carbon Trading Mechanism **(b)** Uniform Carbon Trading Mechanism

Figure 10: Effects of carbon base prices on carbon emissions and total system cost

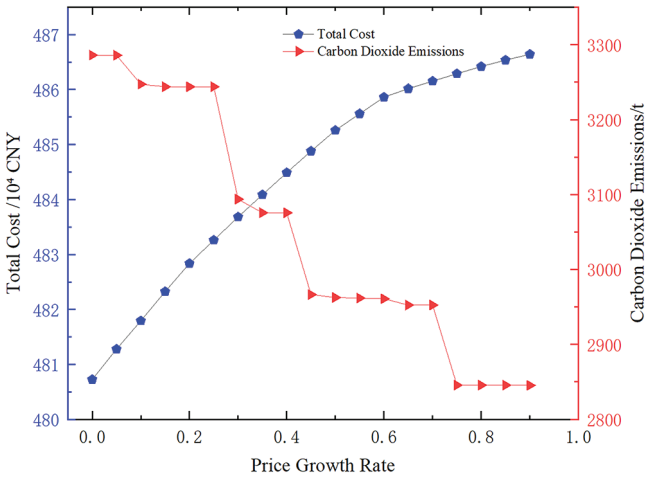

Figure 11: Total cost and carbon emissions under varying price growth rates

Previous studies looked at the effects of base price and growth rate independently on cost dynamics and carbon emissions. Fig. 12 shows atmospheric CO_2 emissions across different growth rates and base price levels to examine the combined impact of these factors. When the base price is low, CO_2 emissions remain relatively low. As the base price increases, CO_2 emissions generally show a downward trend. For instance, when the price growth rate is within [0.2, 0.4], increasing the base price from 100 CNY to 160 CNY reduces CO_2 emissions from approximately 3300.081 t to 3250.192 t. The influence of price growth rate on CO_2 emissions varies across different base price levels. At a base price of 150 CNY, when the price growth rate rises from 0 to 0.4, system CO_2 emissions decrease from 3287.410 t to 3247.160 t. The coordinated regulation of reasonable benchmark prices and price increase rates can effectively mitigate system-level carbon emissions.

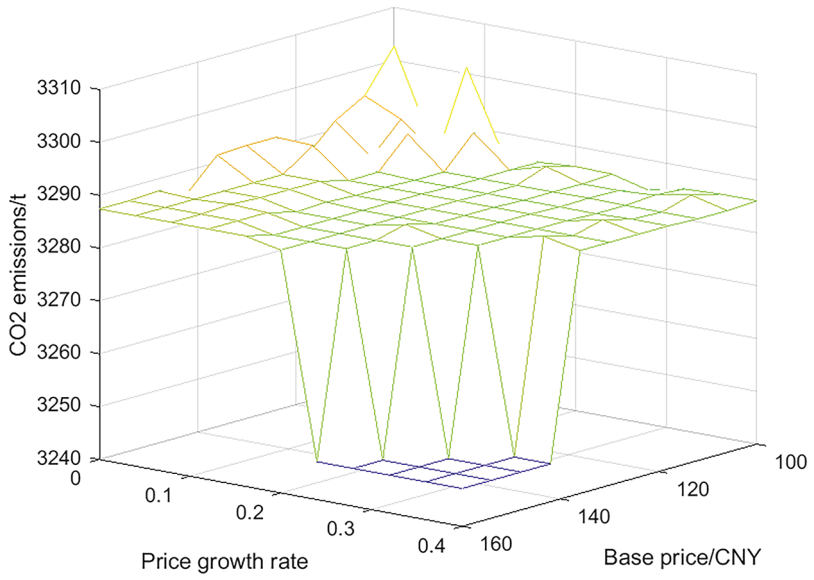

Figure 12: CO_2 emissions under varying base prices and price growth rates

Fig. 13 illustrates the relationship between the compensation coefficient and total cost and CO_2 emissions. When the compensation coefficient rises from 0 to 1, the total cost sharply drops from 5,511,890 CNY to around 2,000,860 CNY. In contrast, system carbon emissions under the tiered carbon trading mechanism exhibit little fluctuation at lower compensation coefficients but undergo a significant decrease from 3243.85 t to 2847.40 t when the compensation coefficient reaches 0.8, after which they stabilize. This indicates that adjusting the compensation coefficient can effectively reduce both total costs and CO_2 emissions, achieving dual improvements in economic efficiency and environmental benefits.

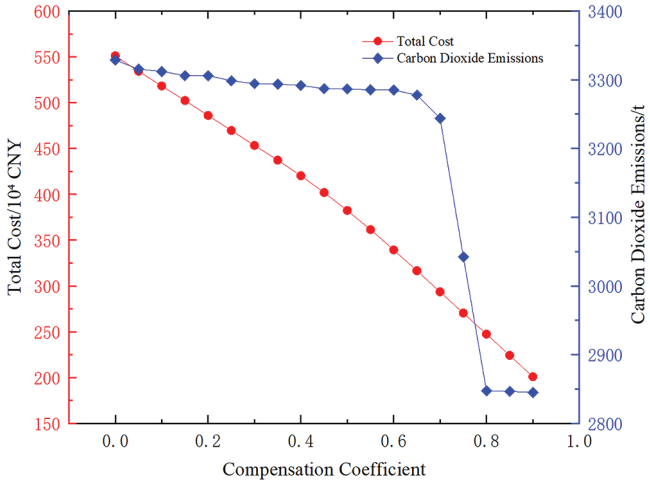

Figure 13: Total cost and CO_2 emissions under different compensation coefficients

4.5 Impact Analysis of Energy and Carbon Prices

In the sensitivity analysis of energy prices and carbon prices on system dispatch outcomes, by adjusting the coal price ratio, natural gas price ratio, and carbon price ratio (within a range of 0.8 to 1.2 times the baseline values), the simulation results in Fig. 14 demonstrate the following:

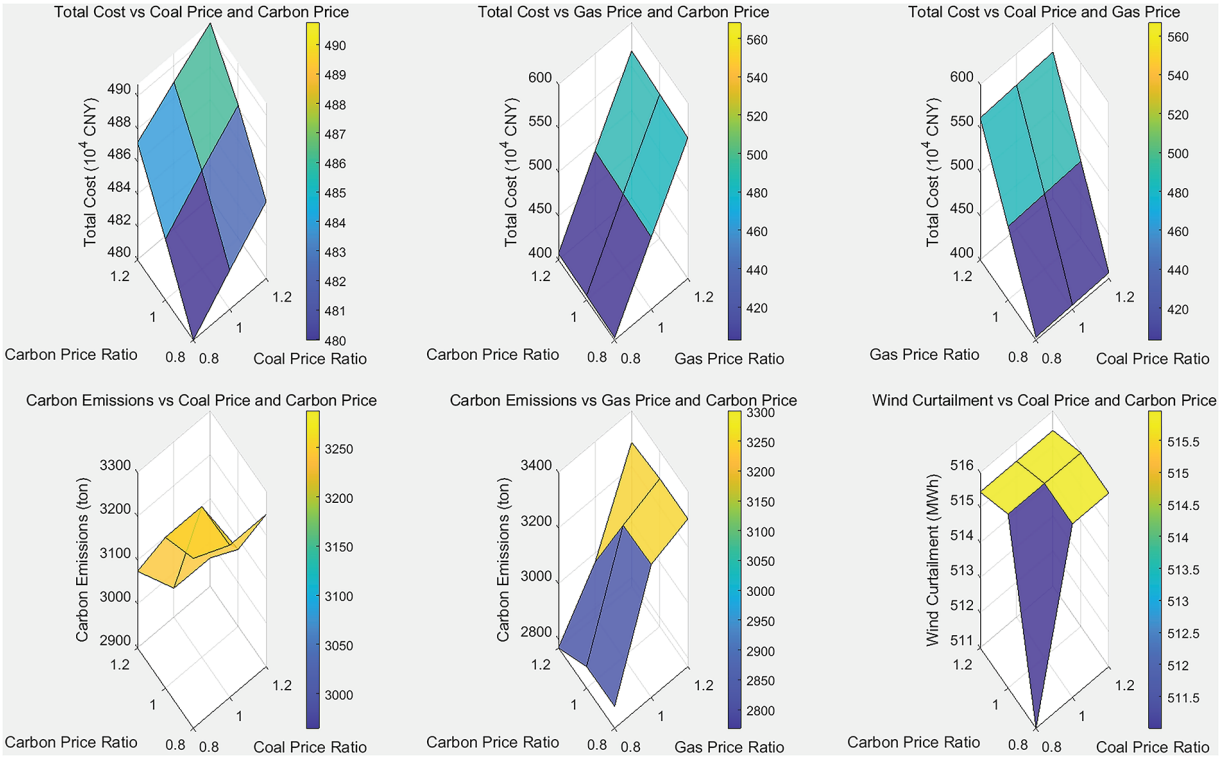

Figure 14: Impacts of carbon, natural gas, and coal prices on system dispatch

Carbon Price is the most effective driver for system emissions reduction. As shown in Fig. 13, an increase in the carbon price ratio consistently leads to a significant reduction in system carbon emissions across all scenarios. For instance, when the coal price ratio is fixed at 1.0, an increase in the carbon price ratio from 0.8 to 1.2 results in a decrease in system carbon emissions from approximately 3175 t to about 3000 t, representing a reduction of nearly 5%. This is primarily because a higher carbon price, through the carbon trading cost mechanism, incentivizes the system to prioritize the dispatch of low-carbon units and enhances the operational intensity of carbon capture systems.

Natural Gas Price is the primary determinant of the total system cost. The analysis indicates that the total cost is far more sensitive to changes in natural gas prices than to coal prices. When the natural gas price ratio increases from 0.8 to 1.2, the total system cost rises rapidly, with an increase of 37.5%. This suggests that, as a key flexible energy source in the system, the procurement cost of natural gas directly influences operational economics.

Coal Price has a relatively limited impact on the overall system. Compared to carbon and natural gas prices, fluctuations in coal prices exhibit weaker effects on both total cost and carbon emissions. An interesting observation is that a slight increase in coal prices is accompanied by a marginal reduction in carbon emissions. This may be attributed to the fact that higher coal prices suppress the output of coal-fired units, prompting the system to increase the share of natural gas or renewable energy in power generation.

The system demonstrates excellent stability in renewable energy accommodation. Across various price scenarios, wind curtailment remains within an extremely narrow range of 511.5 to 516 MWh. This validates that the integrated energy system (IES) model incorporating P2G-CCS coupling, as proposed in this paper, effectively withstands fluctuations in energy market prices and maintains efficient and stable wind power integration capabilities.

5 Conclusion

This study developed and validated an optimal scheduling model for an Integrated Energy System (IES) that synergistically incorporates P2G-CCS coupling, hydrogen-blended natural gas, and a tiered carbon trading mechanism. Our findings demonstrate that these components do not operate in isolation but function as an interconnected system, generating significant synergistic value that achieves both economic and environmental objectives.

The synergistic mechanisms within the proposed system are threefold: First, the P2G-CCS coupling establishes an internal "capture-to-utilization" carbon cycle, converting CO_2 emissions from fossil generation into substitute natural gas, which simultaneously reduces carbon at the source and lowers gas procurement costs. Second, hydrogen blending provides a flexible, dual-use pathway for the hydrogen produced by P2G: it can be directly injected for low-carbon combustion in gas turbines and boilers, or serve as a feedstock for methanation. This flexibility drastically enhances the system's capability to absorb wind curtailment and adapt to varying operational conditions. Finally, the tiered carbon trading mechanism acts as a powerful economic lever, where its punitive higher prices incentivize CCS operation to minimize net emissions, while its compensatory rewards make low-carbon actions like P2G and hydrogen blending economically optimal.

5.1 The Key Findings of This Study Quantitatively Affirm This Synergistic Value

(1) P2G-CCS coupling enables CO_2 recycling to reduce gas procurement, reducing operating costs by 59.3% compared to systems without P2G-CCS coupling and lowering carbon emissions by 3306.307 t. This indicates that the low-carbon economic benefits of the system are enhanced by P2G-CCS coupling.

(2) The study confirms the low-carbon and cost-effective advantages of hydrogen-blended natural gas. Analysis shows that the total cost declines gradually when the hydrogen blending ratio exceeds 14% for gas boilers and reaches 18% for gas turbines. In the meantime, once the hydrogen blending ratio surpasses 12%, the trend of CO_2 emissions decreasing plateaus, even showing an upward tendency. Compared to fixed hydrogen blending ratios, variable ratios reduce gas unit output and electrolysis power consumption by 6.88% and 20.93%, respectively, effectively resolving the forced output constraints caused by fixed blending ratios.

(3) The tiered carbon trading mechanism lowers carbon emissions by 256.801 t and system costs by 313,520 CNY as compared to uniform carbon trading techniques, indicating that tiered carbon trading combined with carbon capture can simultaneously reduce emissions and generate economic benefits. Analyzing tiered carbon trading parameters reveals that adjusting compensation coefficients effectively reduces total costs and carbon emissions. Appropriate base prices and price growth rates further decrease the system's total costs and carbon emissions.

5.2 Practical and Policy Implications

The insights from this research offer clear implications for practitioners and policymakers: For system operators and energy companies, our results provide a strong justification for the strategic, integrated investment in P2G-CCS infrastructure and hydrogen-ready equipment. Future IES planning should prioritize the co-deployment of these technologies to harness their synergistic benefits. Furthermore, adopting dynamic hydrogen blending strategies is key to maximizing operational gains.

For policymakers and regulators, this study validates that well-designed carbon market mechanisms are critical for unlocking technological synergies. We recommend incorporating incentive-punishment tiered structures, similar to the one proposed, into carbon market rules. Carefully calibrating parameters like the

base price, price growth rate, and compensation coefficient can effectively guide capital towards critical low-carbon technologies like P2G, CCS, and hydrogen, thereby accelerating the decarbonization of the entire energy system.

5.3 Future Work

Future research will build upon this work in several directions:

(1) System Expansion: Integrating the transportation and industrial sectors to model a broader hydrogen economy, and extending the scheduling horizon to seasonal or annual scales.
(2) Hydrogen Infrastructure: Modeling the complete hydrogen supply chain, including storage and transportation costs, and analyzing the feasibility of higher hydrogen blends in existing gas networks.
(3) Uncertainty Modeling: Incorporating technological learning curves for cost projections and employing advanced stochastic optimization to handle uncertainties in renewables and prices

Acknowledgement: I would like to express my heartfelt gratitude to the other authors for their invaluable contributions and assistance in this research work.

Funding Statement: The authors received no specific funding for this study.

Author Contributions: The authors confirm their contribution to the paper as follows: Yupeng He: Writing—original draft, methodology, conceptualization. Yansen Sun: Writing—review & editing, methodology, conceptualization, writing—original draft. Yi Ding: Writing—original draft, methodology. Hualei Cui: Writing—review & editing, validation, data curation. Yuanchao Hui: Investigation, conceptualization, supervision. All authors reviewed the results and approved the final version of the manuscript.

Availability of Data and Materials: The authors ensure the authenticity and validity of the materials and data inthe article.

Ethics Approval: Not applicable.

Conflicts of Interest: The authors declare no conflicts of interest to report regarding the present study.

References

1. Zhao X, Ma X, Chen B, Shang Y, Song M. Challenges toward carbon neutrality in China: strategies and countermeasures. Resour Conserv Recycl. 2022;176(1):105959. doi:10.1016/j.resconrec.2021.105959.
2. Xiao D, Lin Z, Wu Q, Meng A, Yin H, Lin Z. Risk-factor-oriented stochastic dominance approach for industrial integrated energy system operation leveraging physical and financial flexible resources. Appl Energy. 2025;377(8):124347. doi:10.1016/j.apenergy.2024.124347.
3. Rubaszek M, Szafranek K. The European energy crisis and the US natural gas market dynamics: a structural VAR investigation. Int Econ Econ Policy. 2024;22(1):11. doi:10.1007/s10368-024-00636-6.
4. Bukar AM, Asif M. Technology readiness level assessment of carbon capture and storage technologies. Renew Sustain Energy Rev. 2024;200(Sep):114578. doi:10.1016/j.rser.2024.114578.
5. Yang C, Dong X, Wang G, Lv D, Gu R, Lei Y. Low-carbon economic dispatch of integrated energy system with CCS-P2G-CHP. Energy Rep. 2024;12:42–51. doi:10.1016/j.egyr.2024.05.055.
6. Asadi J, Kazempoor P. Advancing power plant decarbonization with a flexible hybrid carbon capture system. Energy Convers Manag. 2024;299:117821. doi:10.1016/j.enconman.2023.117821.
7. Yin L, Tao M. Balanced broad learning prediction model for carbon emissions of integrated energy systems considering distributed ground source heat pump heat storage systems and carbon capture & storage. Appl Energy. 2023;329(5):120269. doi:10.1016/j.apenergy.2022.120269.

8. Li X, Li T, Liu L, Wang Z, Li X, Huang J, et al. Operation optimization for integrated energy system based on hybrid CSP-CHP considering power-to-gas technology and carbon capture system. J Clean Prod. 2023;391(9):136119. doi:10.1016/j.jclepro.2023.136119.
9. Khan MW, Wang J, Ma M, Xiong L, Li P, Wu F. Optimal energy management and control aspects of distributed microgrid using multi-agent systems. Sustain Cities Soc. 2019;44(1):855–70. doi:10.1016/j.scs.2018.11.009.
10. Qin L, Ma H, Huang C, Li H, Wu S, Wang G. Low-carbon operation optimization of integrated energy system considering CCS-P2G and multi-market interaction. Front Energy Res. 2024;11:1337164. doi:10.3389/fenrg.2023.1337164.
11. Fan J, Zhang J, Yuan L, Yan R, He Y, Zhao W, et al. Deep low-carbon economic optimization using CCUS and two-stage P2G with multiple hydrogen utilizations for an integrated energy system with a high penetration level of renewables. Sustainability. 2024;16(13):5722. doi:10.3390/su16135722.
12. Zhou D, Yan S, Huang D, Shao T, Xiao W, Hao J, et al. Modeling and simulation of the hydrogen blended gas-electricity integrated energy system and influence analysis of hydrogen blending modes. Energy. 2022;239(10):121629. doi:10.1016/j.energy.2021.121629.
13. Morrone B, Unich A. Numerical investigation on the effects of natural gas and hydrogen blends on engine combustion. Int J Hydrog Energy. 2009;34(10):4626–34. doi:10.1016/j.ijhydene.2009.01.005.
14. Cecere D, Giacomazzi E, Di Nardo A, Calchetti G. Gas turbine combustion technologies for hydrogen blends. Energies. 2023;16(19):6829. doi:10.3390/en16196829.
15. Jin H. A novel gas turbine cycle with hydrogen-fueled chemical-looping combustion. Int J Hydrogen Energy. 2000;25(12):1209–15. doi:10.1016/s0360-3199(00)00032-x.
16. De Robbio R. Innovative combustion analysis of a micro-gas turbine burner supplied with hydrogen-natural gas mixtures. Energy Proc. 2017;126(11):858–66. doi:10.1016/j.egypro.2017.08.291.
17. Chen DY, Liu F, Liu S. Optimal dispatch of virtual power plant integrating P2G-CCS coupling and hydrogen-blended natural gas based on stepwise carbon trading. Power Syst Technol. 2022;46(6):2042–54. (In Chinese). doi:10.13335/j.1000-3673.pst.2021.2177.
18. Liu B, Ding CJ, Hu J, Su Y, Qin C. Carbon trading and regional carbon productivity. J Clean Prod. 2023;420(3):138395. doi:10.1016/j.jclepro.2023.138395.
19. Sun P, Hao X, Wang J, Shen D, Tian L. Low-carbon economic operation for integrated energy system considering carbon trading mechanism. Energy Sci Eng. 2021;9(11):2064–78. doi:10.1002/ese3.967.
20. Namvar A, Salehi J. Multi-objective robust optimization for optimal operation of gas-electricity networks with the penetration of integrated P2G and electric vehicle parking lots. Sustain Cities Soc. 2024;115(2):105826. doi:10.1016/j.scs.2024.105826.
21. Zhang M, Yang J, Yu P, Tinajero GDA, Guan Y, Yan Q, et al. Dual-Stackelberg game-based trading in community integrated energy system considering uncertain demand response and carbon trading. Sustain Cities Soc. 2024;101(2):105088. doi:10.1016/j.scs.2023.105088.
22. Wang R, Wen X, Wang X, Fu Y, Zhang Y. Low carbon optimal operation of integrated energy system based on carbon capture technology, LCA carbon emissions and ladder-type carbon trading. Appl Energy. 2022;311(7):118664. doi:10.1016/j.apenergy.2022.118664.
23. Yang P, Jiang H, Liu C, Kang L, Wang C. Coordinated optimization scheduling operation of integrated energy system considering demand response and carbon trading mechanism. Int J Electr Power Energy Syst. 2023;147(6):108902. doi:10.1016/j.ijepes.2022.108902.
24. Nie Q, Zhang L, Tong Z, Dai G, Chai J. Cost compensation method for PEVs participating in dynamic economic dispatch based on carbon trading mechanism. Energy. 2022;239:121704. doi:10.1016/j.energy.2021.121704.
25. Zhang Y, Zhang P, Du S, Dong H. Economic optimal scheduling of integrated energy system considering wind-solar uncertainty and power to gas and carbon capture and storage. Energies. 2024;17(11):2770. doi:10.3390/en17112770.
26. Götz M, Lefebvre J, Mörs F, McDaniel Koch A, Graf F, Bajohr S, et al. Renewable power-to-gas: a technological and economic review. Renew Energy. 2016;85(4):1371–90. doi:10.1016/j.renene.2015.07.066.

27. Fan W, Cui S, Li H. Bi-level optimal scheduling of integrated energy system considering two-stage power-to-gas and hydrogen blending in natural gas. Elect Measure Instrument. 2025;62(2):16–25. (In Chinese). doi:10.19753/j.issn1001-1390.2025.02.003.
28. Yu X, Hu ZJ, Chen JP, Yan GZ, Gong HS, Wu JH. Optimal dispatch of integrated energy system considering P2G-CCS and supply-demand flexible response under stepped carbon. Eng J Wuhan Univ. 2024;57(10):1360–71. (In Chinese). doi:10.14188/j.1671-8844.2024-10-002.
29. Xie T, Wang Q, Zhang G, Zhang K, Li H. Low-carbon economic dispatch of virtual power plant considering hydrogen energy storage and tiered carbon trading in multiple scenarios. Processes. 2024;12(1):90. doi:10.3390/pr12010090.